4.9 MICROMETEOROLOGICAL CHARACTERISTICS OF THE SEA BREEZE DURING THE WILMINGTON 2005 URBAN DISPERSION STUDY

Xiangyi Li and Marko Princevac *
Department of Mechanical Engineering, University of California, Riverside, CA

The urban dispersion study took place in Wilmington, California, in June 2005, with the main goal to facilitate evaluation and improvement of a newly developed urban dispersion model for the California Air Resources Board. The meteorological equipment consisting of mini-sodars, sonic anemometers, a hygrometer, a microwave temperature profiler and energy balance instruments was deployed at the release site and another site located four kilometers inland. This instrumentation setup enabled investigations of the micrometeorological characteristics related to the interactions between the marine and urban boundary layers. The days with offshore synoptic winds were taken into the consideration when the distinct sea breeze pattern can be discerned from the ambient flows. The sea breeze layer depth and the convective internal boundary layer depth were determined from the remote sensing measurements and compared to the theoretical models. The micrometeorological characteristics of the sea breeze front in the surface layer were analyzed from the mean wind and turbulence properties. The contributions to the turbulence energy dissipation from the mechanical and thermal effects were discussed.

1. INTRODUCTION

The urban dispersion study took place in Wilmington of the Los Angeles County, California, in June 2005, with the main goal to facilitate evaluation and improvement of a newly developed urban dispersion model for the California Air Resources Board (CARB). The tracer gas was released from the power plant located in the vicinity of the Los Angeles Harbor. The tracer samplers were positioned along three arcs: one, three and five kilometers from the release point. Each sampling arc had 16 samplers positioned 6 degrees apart. At the same time, the meteorological equipment consisting of mini-sodars, sonic anemometers, a hygrometer, a microwave temperature profiler and energy balance instruments was deployed at the release site and another site located four kilometers inland. This instrumentation setup not only provided turbulent parameters for the dispersion model, but also enabled investigations of the micrometeorological characteristics specific for the shoreline urban environment. We are particularly interested in the interactions between the marine and urban boundary layers. Thanks to the intensive ground heating by solar radiation the summer is the best time to study the sea breeze and its impact on the urban coastal environment. Sea breezes play an important role in modifying the urban environments by bringing the cool and moist marine air mass from the marine boundary layer.

The Sea breeze is a mesoscale meteorological phenomenon which has been studied for many centuries, and extensively in the recent several decades. Rotunno [1983] presented a critical review in the linear models of sea and land breeze and developed a simple model which was followed and further developed (e.g. Dalu and Pielke [1989]). Numerical modeling was also carried out by many researchers in two dimensions (e.g. Estoque [1962]) and in three dimensions (e.g. Pielke [1974]). Laboratory simulations also provide good information on the gravity current nature of the sea breeze, such as the laboratory researches reviewed by Simpson [1997]. And above all, the filed experiments are major approach in studying the sea breeze, which all other studies are based on. The filed experimental progress was made using traditional instrumented tower, balloons and aircrafts, remote sensing including radars [Atlas 1960], sodars (SOund Detection And Ranging, and lidars (Light Detection And Ranging) [Banta et al. 1993]. Most of these studies, both measurements and simulations, focus on the mesoscale meteorological characteristics in the atmospheric boundary layer and the free atmosphere above. However, the microscale meteorological characteristics related to the turbulent structure of the sea breeze were given less attention. In this paper, we used the meteorological data collected from the Wilmington 2005 to study the micrometeorological properties of the sea breeze, especially in the surface layer where most urban activities take place.

2. INSTRUMENTATION SETUP

The meteorological instrumentations were deployed at 2 sites near the coastal line of Los Angeles County, California, one at the release site inside the facilities of the Department of Water and Power (referred to as DWP) near the Los Angeles Harbor, another located 4 kilometers inland at the Los Angeles County Joint Water Pollution Control Plant (LA County Sanitation Station, referred to as LAS). Please refer to the map in Figure 1 (located at the end of paper, after references) for the site locations and the GPS information.

The instrumentations at DWP included one mini-sodar (Atmospheric Systems) and a trailer carrying a 10-meter tower equipped with two sonic anemometers (Campbell Sci. CSAT3, 3.1m AGL and 6m AGL), one krypton hygrometer (Campbell Sci. KH20, 3.1m AGL), one net radiometer (Kipp and Zonen CNR1, 10.2m AGL), one temperature and relative humidity (RH) probe (Vaisala HMP45C-L, 1.25m AGL), and one infra-red (IR) thermocouple (Apogee IRTS-P, 1.25m AGL). During the limited period, two aerosol monitors (TSI

* *Corresponding author address:* Marko Princevac, Dept. of Mech. Engr., Univ. of Calif., Riverside, CA 92507; email: marko@engr.ucr.edu

DustTrak8520) were also deployed for particular matter (PM) measurements. Please refer to Figure 2 for the instrumentations on the tower and their heights above ground level (AGL).

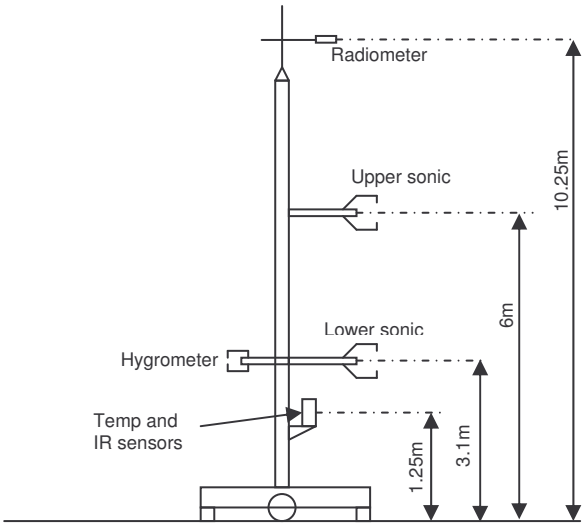

Figure 2 - Schematic of the instrumented tower at DWP

The instrumentations at LAS included one mini-sodar (Atmospheric Systems), one microwave temperature profiler (Kipp and Zonen MTP-5), and one sonic anemometer (Campbell Sci. CSAT3). The sonic was mounted on a tripod on the roof of a small building (7m AGL, and 2.25m above the roof level). The sonic anemometers stored 10 Hz data and both mini-sodars stored raw moment data every 2-4 seconds. All other instruments stored 5 min averaged data. The sonic and sodar moment data were averaged properly into 5 min and 1 hour averaged data files for the analysis in this paper.

3. STRUCTURE OF SEA BREEZE LAYER AND CONVECTIVE INTERNAL BOUNDARY LAYER

A sea breeze system consists of the following components [Miller et al. 2003]: sea breeze circulation (SBC), sea breeze gravity current (SBG), sea breeze front (SBF), sea breeze head (SBH), Kelvin-Helmholtz billows (KHB), and convective internal boundary layer (CIBL). In this section we focus on the overall structure of the sea breeze layer (SBL, within which the SBG develops with the upper limit as the SBH and the KHB) and CIBL. The surface layer micrometeorological characteristics of the SBF will be discussed in details in Section 4.

As a typical day with distinct sea breeze pattern, June 26, 2005 was chosen for analysis in this paper. The synoptic wind was mainly northern or northwestern. During summertime in southern California, the North American monsoon blows eastwards from the ocean to the continent due to the synoptic pressure gradient. The Coriolis force deflects this monsoon making it northerly/northwesterly in Wilmington. This offshore flow confronts the sea breeze currents in the opposite direction, and makes it easier to distinguish the sea breeze from the ambient flows. The local sunrise time was 0545 PDT (pacific daylight time) and the sunset time was 2010 PDT.

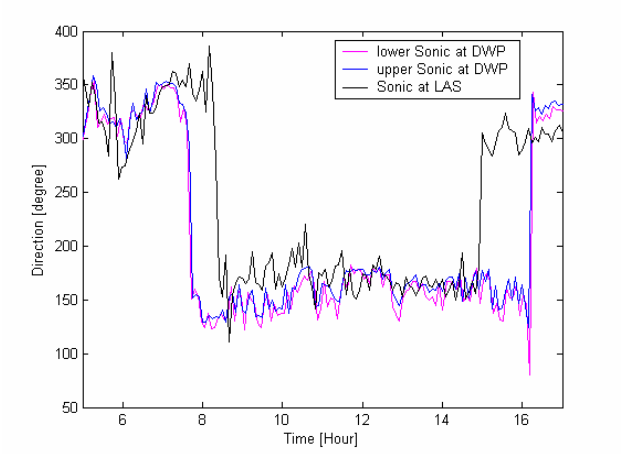

Figure 3 - Wind directions from sonics on 6/26/2005

Figure 3 shows the wind directions of both sites from sonic anemometers. From the wind direction shift it is indicated that the SBF arrived at DWP around 0740 PDT and at LAS around 0815 PDT. The wind shift in the afternoon began at LAS around 1500 PDT and at DWP around 1610 PDT due to the weakening of sea breeze and the turn back of the prevailing offshore wind. It is also observed that the wind shifted counterclockwise when the sea breeze arrived and shifted clockwise when the prevailing offshore wind overcame the sea breeze. This cannot be explained by the effect of the Coriolis force on the northern hemisphere. This can be contributed to the prevailing offshore flow from the north-northwest. It is also observed that the topography of coastline plays significant role. The wind direction of the sea breeze we observed was 160 degrees at DWP, and 170 degrees at LAS, respectively. This is due to the mountains west to Wilmington which serve as a shield to greatly undermine the impact of the west wind generated from the Pacific Ocean on the south wind generated from the Pedro Bay. Please refer to Figure 1 for more information on local topography.

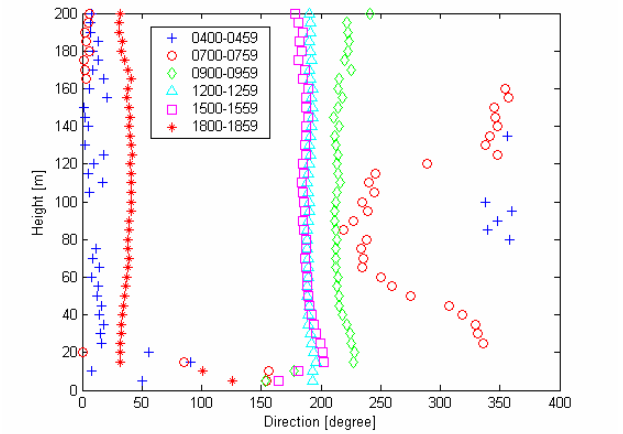

Figure 4 - Wind direction from mini-sodar at DWP on 6/26/2005

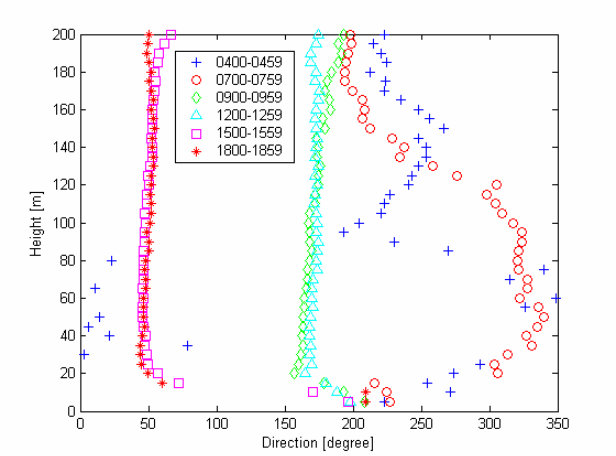

Figure 5 - Wind direction from mini-sodar at LAS on 6/26/2005

The remote sensing instruments including sodars and MTP-5 can provide the overall information of the SBL and the CIBL. The sodars gave velocity measurements up to 200m with a resolution of 5m, while the MTP-5 gave temperature measurements up to 600m with a resolution of 50m. Figure 4 and 5 show the wind directions from both sites on June 26. It can be seen that after 0900 PDT, the wind directions at both sites completed the shift to sea breeze up to 200m. So it is indicated that the sea breeze layer extends above 200m.

Figure 6 shows the potential temperature profiles from MTP-5 at LAS on June 24, 2005, which are representative profiles for most of the days during the Wilmington experiment. It is believed that after the first inversion above the ground level which marks the CIBL depth, the height where the potential temperature gradient vanishes marks the SBL depth. We never saw such a dramatic decrease in potential temperature gradient above the CIBL and up to 600m for most days. So it is proposed the SBL depth is greater than 600m. However, June 26 turned out to be an exception. Figure 7 shows the potential temperature profiles on June 26. It is indicated the SBL depth was approximately 350 m on this day.

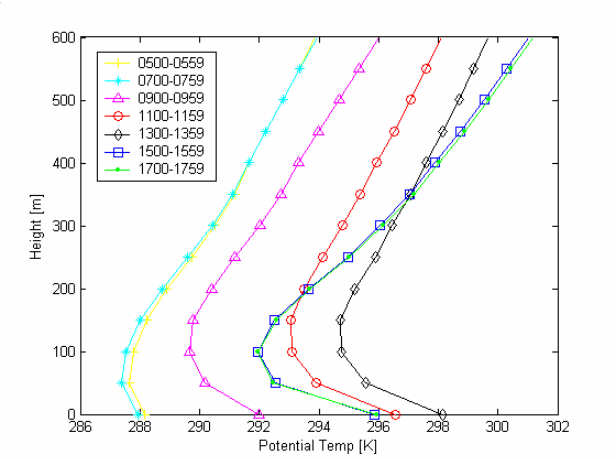

Figure 6 - Potential Temperature Profile from MTP-5 on 06/24/2005

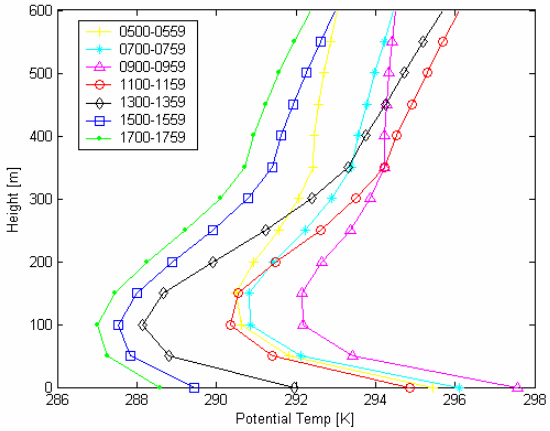

Figure 7 - Potential Temperature Profile from MTP-5 on 06/26/2005

In order to estimate the SBL depth, we use the equation of sea breeze penetration proposed by Simpson and Britter [1980]

$$|U| = 0.62\sqrt{\frac{\Delta T}{T} gh} - 0.59u_g \qquad (1)$$

where ΔT is the temperature difference between the land and the sea, h is the mean SBL depth, u_g is the cross-shore geostrophic wind component.

In order to determine the penetration speed of the sea breeze, we calculated the penetration time from DWP to LAS to be 35 minutes from Figure 3. We use the following equation to estimate the penetration speed of the SBF to be 2.53 m/s. (Δt is the penertration time, L is the distance between DWP and LAS, and α is the angle between the mean wind direction and the straight line connecting DWP and LAS)

$$|U| = \frac{L}{\Delta t \cdot \cos\alpha} \qquad (2)$$

After substituting U into equation (1), using ΔT=3K, T=293K, g=9.8m/s^2, u_g=0.65m/s, the mean depth of SBL was estimated to be only 136m, which turns out to be a poor theoretical prediction.

From MTP-5 potential temperature profile, the CIBL depth at LAS was estimated to be from 50m to 150m on June 26. For comparison to theoretical results, we use the CIBL growth equation by Venkatram [1977]

$$h = \sqrt{\frac{2C_D x\Delta\theta}{\gamma(1-2E)}} \qquad (3)$$

where h is the CIBL depth, C_D is the friction coefficient, x is the distance from the shoreline, $\Delta\theta$ is the potential temperature difference between the land and the sea, γ is the lapse rate above the CIBL, E is the entrainment coefficient. Using C_D=0.012, x=6000m, $\Delta\theta$=3K, γ=0.007K/m, E =0.08, the CIBL depth at LAS was calculated to be 271m, which overestimated the result.

The disagreements between the theoretical models and our experimental results are not surprising due to the simplicity of these models. It is suggested that more accurate and universal but still sufficiently simple

models of the SBL and the CIBL growth are needed for the future studies.

4. SURFACE LAYER CHARACTERISTICS OF SEA BREEZE FRONT

Data from sonic anemometers, radiometer, temperature and IR probe, etc. provide good information of the micrometeorological characteristics of the sea breeze in the surface layer which is the lowest part of the atmospheric boundary layer where most of urban activities take place. Here we use these data to study the change in turbulent characteristics associated with the arrival of the SBF.

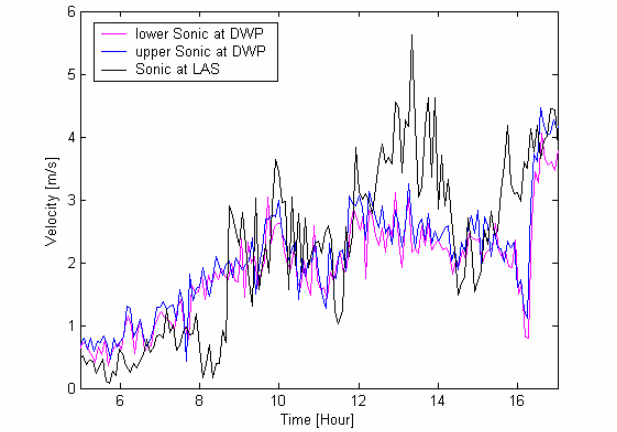

Figure 8 - Horizontal wind speed from sonics on 6/26/2005

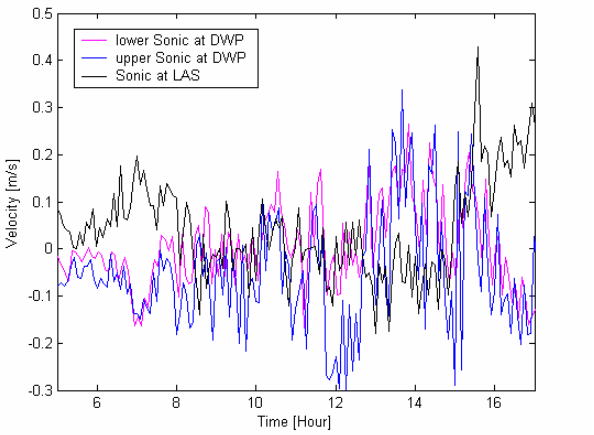

Figure 9 - Vertical wind component from sonics on 6/26/2005

The horizontal wind speed, vertical wind component, temperature, and turbulence kinetic energy (TKE) from sonic anemometers at both sites on June 26 were shown in Figures 8, 9, 10, and 11. According to Chiba [1993], with the arrival of the SBF, the wind shifts with a drop in temperature and a minimum in wind speed. It is observed in our case with the wind shift, the wind speeds did decrease and then pick up but the temperature did not drop. The explanation is that the contribution of strong sun heating overcomes that of the cold marine air flow. But we did observe the decrease in temporal temperature gradient. After the passage of the SBF, the temperature increased slower, with the evidence of sharply decrease in slopes of temperatures from approximately 1.5°C/h (Figure 10 red line) to 0.6°C/h (Figure 10 blue line). Chiba [1993] also stated that the vertical wind velocity experiences a remarkable downdrafts and updrafts immediately before and after the passage of the SBF. In our case, we did not observe such dramatic changes in vertical wind component. The TKE immediately before and after the passage of the SBF also shows a sudden increase, which indicates the increase in the turbulent activity with the arrival of the SBF.

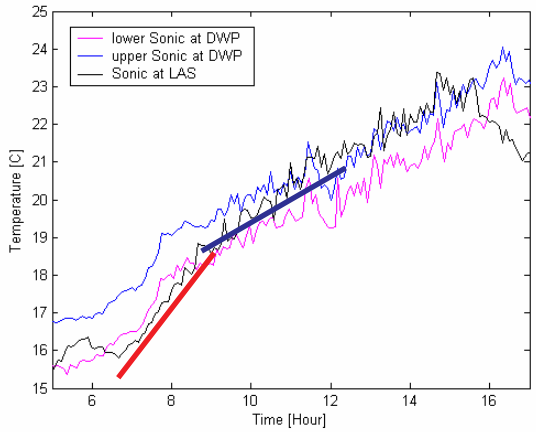

Figure 10 - Temperature from sonics on 6/26/2005

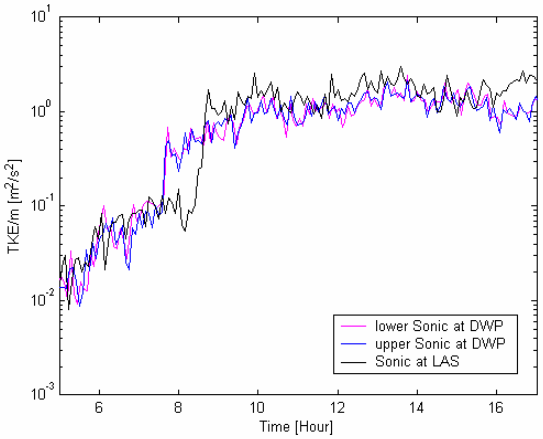

Figure 11 - Turbulence kinetic energy from sonics on 6/26/2005

The turbulence dissipation rate ε was calculated using the Kolmogorov -5/3 law in the inertial subrange,

$$p(f) = C \cdot f^{-5/3} \left(\frac{\varepsilon U}{2\pi} \right)^{2/3} \quad (4)$$

where p is the power spectral density in [m^2/s] calculated from the velocity spectrum, C is the Kolmogorov constant here taken as 0.7, f is the frequency, ε is the dissipation rate to be determined, and U is the wind speed. Figure 12 shows the velocity spectrum

calculated from the fluctuations of *w* component. The solid line is the best fit used for estimation of dissipation rate.

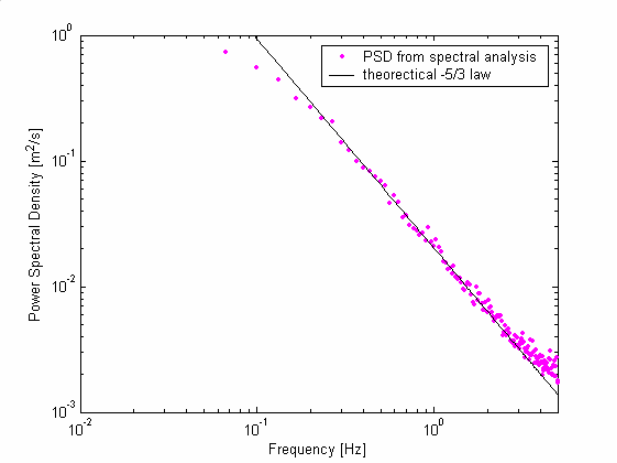

Figure 12 - Velocity spectrum from the lower sonic at DWP on 6/26/2005

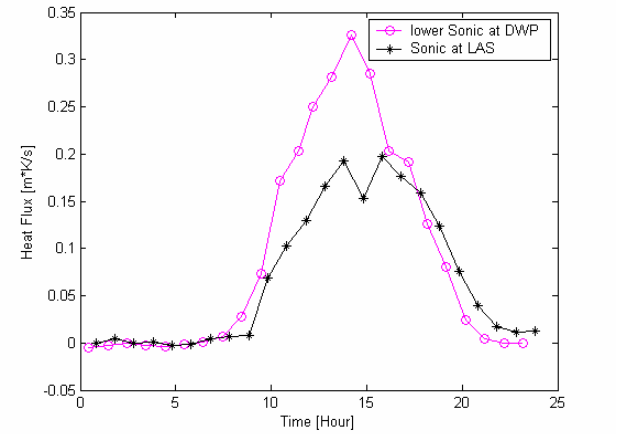

Figure 13 - Sensible heat flux from sonics on 6/26/2005

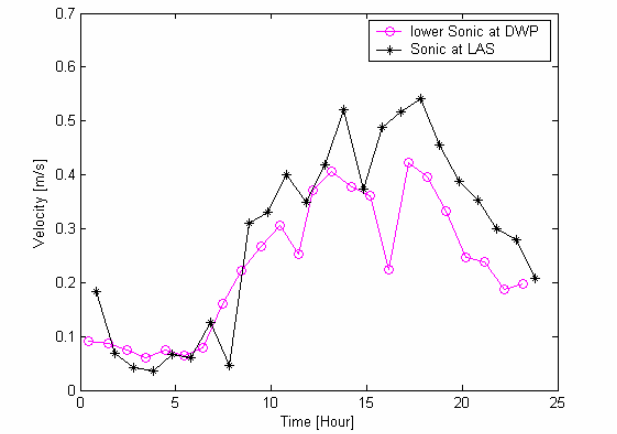

Figure 14 - Frictional velocity from sonics on 6/26/2005

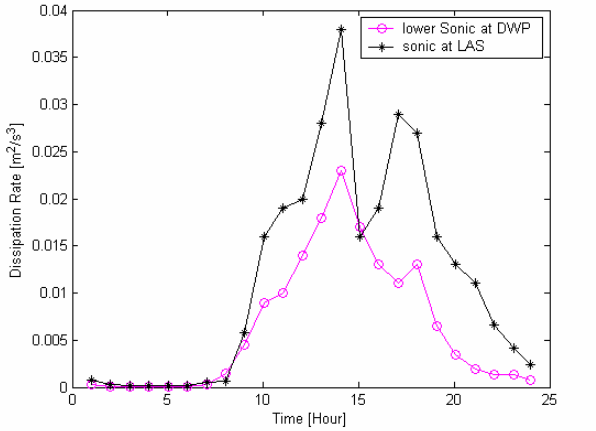

Figure 15 - Turbulence dissipation rate from sonics on 6/26/2005

Figure 13, 14, and 15 show the hourly averaged sensible heat flux, frictional velocity and turbulence dissipation rate calculated from the sonic anemometer data. The dissipation rate follows heat flux. However the sonic at DWP showed a higher heat flux but a lower dissipation rate than sonic at LAS. This is due to the lower frictional velocity at DWP. This confirms that both the shear and the convection contributed to the increase in the turbulence dissipation rate. The strong ground radiation due to sun heating still dominated the turbulent characteristics in the surface layer during the day. Intense shear and convective activity within the SBF led to increase in the turbulence dissipation rate.

5. SUMMARY

The analysis on micrometeorological characteristics in the sea breeze layer, the convective internal boundary layer, and the surface layer was carried out based on the meteorological measurements in Wilmington 2005. The sea breeze layer depth and the convective boundary layer depth were determined from the remote sensing instruments and compared to the simple theoretical models. It is suggested that more accurate and universal models are needed for the future studies. The sea breeze front penetrated inland with a sudden change in the wind direction, the wind speed, the temporal temperature gradient, and the turbulence kinetic energy. The increase in the turbulence dissipation rate was due to both mechanical and thermal effects.

Acknowledgements. The authors would like to thank Mr. Neil Zimmerman for his great work in the field experiments and data processing.

REFERENCES

Atlas, D., 1960: Radar detection of the sea breeze, *J. Meteor.*, **17**, 244-258.

Banta, R. M., L. D. Oliver, and D. H. Levinson, 1993: Evolution of the Monterey Bay sea-breeze layer as

observed by pulsed Doppler lidar, *J. Atmos. Sci.*, **50**, 3959-3982.

Chiba, O., 1993: The turbulent characteristics in the lowest part of the sea breeze front in the atmospheric surface layer, *Bound.-Layer Meteor.*, **65**, 181-195.

Dalu, G. A., and R. A. Pielke, 1989: An analytical study of the sea breeze, *J. Atoms. Sci.*, **46**, 1815-1825.

Estoque, M. A., 1962: The sea breeze as a function of the prevailing synoptic situation, *J. Atmos. Sci.*, **19**, 244-250.

Miller, S. T. K., B. D. Keim, R. W. Talbot et al., 2003: Sea breeze: structure, forecasting, and impacts, *Rev. Geophys.*, **41**, 3, 1-31.

Pielke, R. A., 1974: A three-dimensional numerical model of the sea breezes over South Florida, *Mon. Wea. Rev.*, **102**, 115-139.

Rotunno, R., 1983: On the linear theory of the land and sea breeze, *J. Atmos. Sci.*, **40**, 1999-2009.

Simpson, J. E., and R. E. Britter, 1980: A laboratory model of an atmospheric mesofront, *Q. J. Royal Meteor. Soc.*, **106**, 485-500.

Simpson, J. E., 1997: *Gravity Currents in the Environment and the Laboratory*, 244, Cambridge Univ. Press, New York.

Venkatram, A., 1977: A model of internal boundary layer development, *Bound.-Layer Meteor.*, **11**, 419-437.

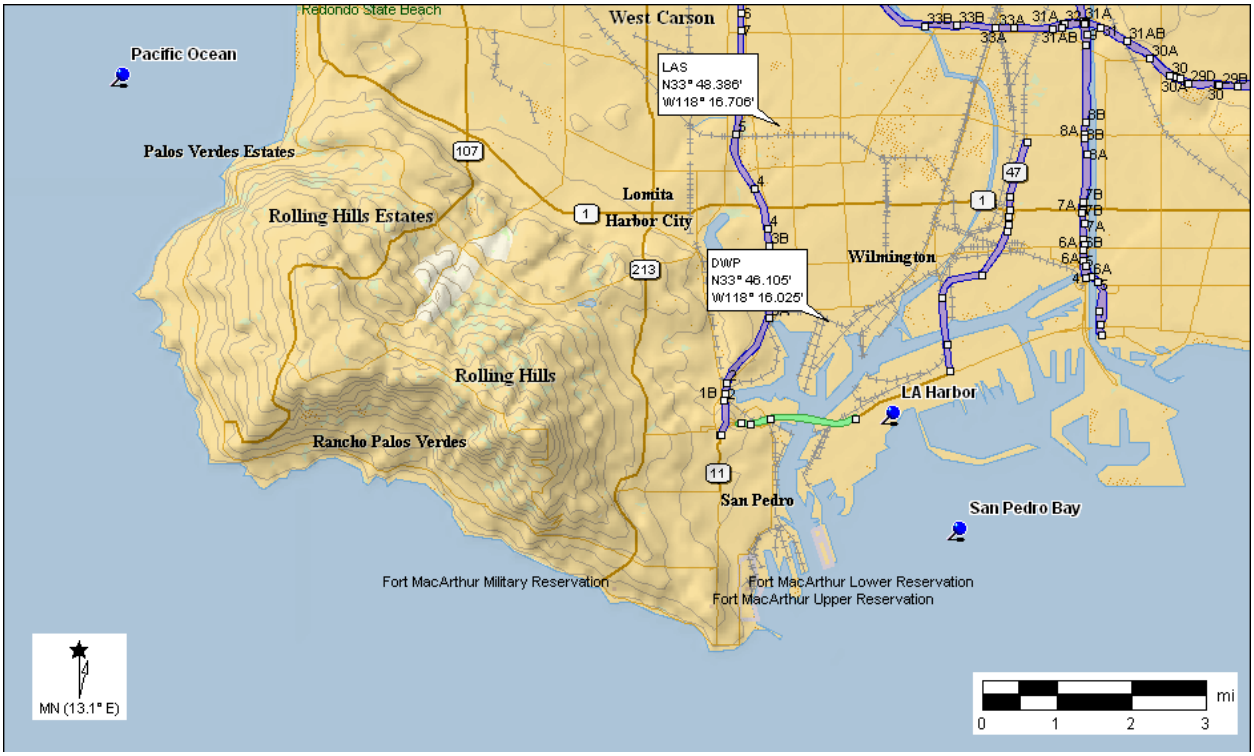

Figure 1 - Sites locations and GPS information